Revista Mexicana de Astronomía y Astrofísica, **40**, 25–30 (2004)

VARIATION OF CENTRAL STAR MASSES IN PLANETARY NEBULAE WITH HEIGHT ABOVE THE GALACTIC PLANE

J. P. Phillips

Instituto de Astronomía y Meteorología
Guadalajara, Jalisco, México

Received 2003 October 15; accepted 2003 November 27

RESUMEN

Hay razones para sospechar que las masas de las progenitoras de las nebulosas planetarias (PNe) disminuyen con la altura sobre el plano galáctico z. Esto implicaría una disminución similar en las masas medias de las estrellas centrales $<M_{CS}>$. Reportamos otra manera de determinar estos gradientes. Mostramos que la distribución de las temperaturas de brillo en 5 GHz de las PNe depende fuertemente de la latitud galáctica b. Esta variación se debe probablemente a un cambio en la función de masa de la estrella central $N(M_{CS})$. Las fuentes a alta b parecen tener una $N(M_{CS})$ con mayor pendiente, lo cual implica que existen pocas PNe con estrellas centrales de masa grande. En contraste, las fuentes a baja b tienen una $N(M_{CS})$ con pendiente menor, lo cual implica un mayor número de PNe con M_{CS} grandes. Mostramos que esto tiene como consecuencia gradientes significativos de la masa media $<M_{CS}>$ con b. Encontramos que $d<M_{CS}>/d|b_{LOW}| \simeq 2.0\times10^{-3}$ $M_\odot$ deg^{-1} para nebulosas con 1.0 $<\log(T_B/\mathrm{K})<$ 3.6, donde $|b_{LOW}|$ es el límite inferior de la latitud de las fuentes. Esto corresponde a un gradiente $d<_{CS}>/d|z_{LOW}|$ $\simeq 5.6\times10^{-2}$ kpc^{-1} para nebulosas con $|z|>|z_{LOW}|$, adoptando las distancias estadísticas de Phillips (2002).

ABSTRACT

There are various reasons for suspecting that the progenitor masses of planetary nebulae (PNe) decline with height z above the Galactic plane. This, if true, would also imply a similar decrease in mean central star masses $<M_{CS}>$. We report here a further way in which such gradients may be determined. It will be shown that the distribution of planetary nebulae with respect to 5 GHz brightness temperature varies strongly with Galactic latitude. This variation is likely to arise from a change in the central star mass function $N(M_{CS})$. High latitude sources appear to have a steeply varying function $N(M_{CS})$, implying the presence of relatively few nebulae with high central star masses. By contrast, the low latitude sources have a much gentler fall-off in $N(M_{CS})$, implying a larger proportion of high M_{CS} nebulae. This is shown to imply significant gradients of mean mass $<M_{CS}>$ with latitude b. We find that $d<M_{CS}>/d|b_{LOW}| \simeq 2.0\times10^{-3}$ $M_\odot$ deg^{-1} for nebulae having 1.0 $<\log(T_B/\mathrm{K})<$ 3.6, where $|b_{LOW}|$ represents the lower limit latitude of the sources. This corresponds to a gradient $d<M_{CS}>/d|z_{LOW}| \simeq 5.6\times10^{-2}$ kpc^{-1} for nebulae with heights $|z|>|z_{LOW}|$, and where one adopts the statistical distances of Phillips (2002).

Key Words: **ISM: JETS AND OUTFLOWS — PLANETARY NEBULAE: GENERAL — STARS: EVOLUTION**

1. INTRODUCTION

There are various reasons to suppose that the mean progenitor masses M_{PG} of planetary nebulae vary with height z above the Galactic plane. Koeppen & Cuisinier (1997), for instance, have found a gradient in the abundances of N and He with Galactic height. Given that that the abundances of PNe are likely to depend upon progenitor mass (e.g., Renzini & Voli 1981; Marigo, Bressan, & Chiosi 1998;

van den Hoek & Groenewegen 1997), then this may suggest a corresponding gradient $d<M_{PG}>/dz$. It has also been demonstrated that PNe having large Galactic latitudes $|b|$ tend to have low mean Zanstra temperatures $<T_Z(\mathrm{He\,II})>$ (Phillips 2003a). This is likely to reflect a tendency for lower mass stars to have lower mean effective temperatures $<T_{\rm eff}>$, and would be consistent with a vertical gradient in central star (and progenitor) masses.

We shall point out in the following that there is at least one further way in which such gradients may be demonstrated. We shall note that the distribution of PNe with respect to 5 GHz brightness temperatures varies as a function of lower limit latitude $|b_{LOW}|$. This can be shown to be consistent with stellar evolutionary theory providing that there is a strong latitude variation in $N(M_{CS})$, the central star mass function. This, in turn, will be shown to imply the presence of gradients $d<M_{CS}>/d|b_{LOW}|$ in central star masses, and will permit us to assign approximate values for $d<M_{CS}>/d|z|$.

2. THE OBSERVED VARIATION IN $N[\log(T_B)]$

We have employed the large sample of brightness temperatures listed by Zhang (1995) to evaluate the trend $N[\log(T_B)]$ for Galactic PNe. These values, corresponding to some 484 nebulae, are limited to sources having Galactic longitudes $10°<l<350°$. It follows that most of these PNe are likely to represent Galactic disk sources, and that the proportion of Galactic bulge nebulae will be relatively small. The distribution of the sources is illustrated in Figure 1 for various lower limit latitudes $|b_{LOW}|$. The lowest curve corresponds to $|b_{LOW}| = 0°$, and represents the distribution $N[\log(T_B)]$ for the entire data sample.

Such trends are open to a variety of biases, of which the most prominent are the following:

1. Most of the PNe are located at small Galactic latitudes b, where levels of interstellar extinction are also appreciable. This extinction will cause a reduction in source detectability where visual (and radio) surface brightnesses are low, and leads to a decline in $N[\log(T_B)]$ as T_B becomes small. Such an effect is likely to be strongly dependent upon Galactic latitude.

2. As visual surface brightnesses decrease, then it becomes increasingly difficult to detect the sources against background sky noise, and as a result of limited instrumental sensitivities. It is difficult to quantify these effects precisely, although trends in Hβ surface brightness suggest reduced levels of sample completeness where $\log(S(H\beta)/\mathrm{erg\ cm^{-2}\ s^{-1}\ arcsec^{-2}}) < -15$, corresponding to temperatures $\log(T_B) < 0$.

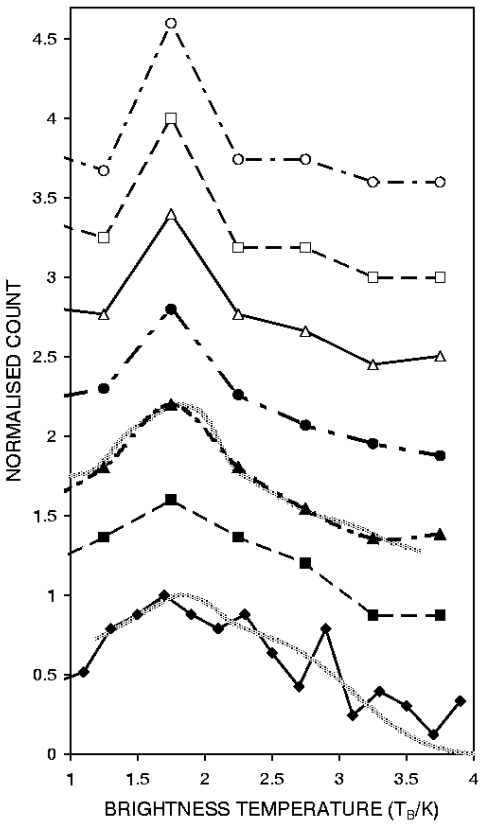

Fig. 1. The variation of observed source numbers as a function of $\log(T_B)$, and lower limit latitude $|b_{LOW}|$. The various curves correspond (bottom to top) to $|b_{LOW}| = 0°$, 2.5°, 5°, 7.5°, 10°, 12.5°, and 15°. They have been normalized and vertically displaced for greater clarity. It will be noted that there is a strong variation in the profiles, such that low latitude sources extend over the full observed range in T_B, whilst high latitude sources are concentrated about $\log(T_B) \simeq 1.75$. Finally, it should be noted that we have only illustrated the range $\log(T_B) > 1$, since it is likely that lower T_B sources are open to strong (and latitude dependent) biases.

3. Finally, we note that radio detection limits occur close to $T_B(\mathrm{LIM}) \simeq 3\sigma(T_B) \simeq 0.04$ K (e.g., Milne 1979; Milne & Aller 1975, 1982), implying a rapid fall-off in sample completeness where $\log(T_B) < -1.4$.

These various biases will affect low brightness temperature sources in particular. We have therefore illustrated trends for higher brightness temperature sources alone (i.e., those having $\log(T_B) > 1.0$). These represent 61% of the complete data set. We shall also restrict our analysis of functions $N(M_{CS})$ to sources lying in the range $1.0 < \log(T_B) < 3.6$ (see § 4).

Even the higher brightness temperature sources are not entirely free from biases, however. Sources having large values of T_B will tend to be observable (and detectable) to larger distances than for other PNe. This will likely result in the relative populations of these sources being over-represented, all other factors remaining equal. On the other hand, it is also likely that high T_B sources are associated with larger mean progenitor masses (see § 3), and this would imply lower mean latitudes, higher levels of extinction, and lower probabilities of source detection. The trends for high T_B sources are therefore subject to conflicting biases, and it is unclear whether they are over- or under-represented in the samples of Zhang (1995) and others (see e.g., Phillips [2002] and Zijlstra, Pottasch, & Bignell [989]).

The trends in $N[\log(T_B]$ are also based upon observations taken with interferometric and single dish surveys, and these have their own biases in terms of radio fluxes and brightness temperatures. Single dish observations (such as those of Milne [1979] and Milne & Aller [1975; 1982]) tend to measure nebulae brighter than $\sim$ 20 mJy, whilst interferometric measures (such as those of Zijlstra et al. [1989]) are biassed towards younger and more compact sources. These various surveys appear to have little overlap in terms of the areas of sky measured.

The sources in the present sample are therefore by no means *complete* in the usual sense of this word; they are not balanced according to nebular size or type. This suggests that the mass functions to be determined later will not be representative of the generality of PNe. On the other hand, such biases as do exist are unlikely to be appreciably latitude dependent, and the variation of $N[\log(T_B)]$ with b is probably indicative of real trends in latitude.

It will be noted from Fig. 1 that the variation of $N[\log(T_B)]$ with $|b_{LOW}|$ is appreciable. Where $|b_{LOW}| = 0$, for instance, then the distribution of sources is broad, and extends over the full observed range in T_B. As values of $|b_{LOW}|$ increase, however, then the distribution $N[\log(T_B)]$ becomes very much narrower, and a large fraction of sources appear to be confined to a range 1.5 $<\log(T_B) < 2.0$. It is therefore apparent that the proportion of high T_B sources declines as $|b_{LOW}|$ increases. Since most high T_B sources correspond to nebulae having high central star masses (see § 3), then the decrease in the proportion of such nebulae implies a variation in $N(M_{CS})$. We shall consider variations in these mass functions later in § 4.

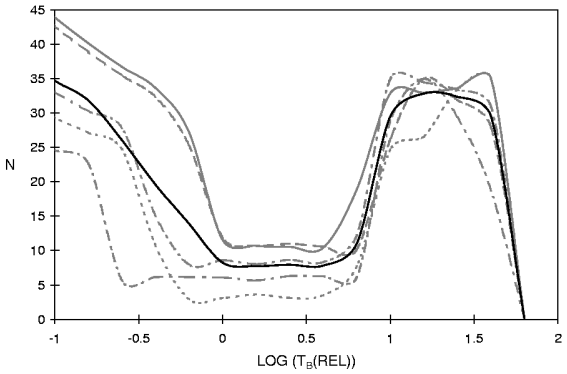

Fig. 2. A superposition of trends $N[\log(T_B), M_{CS}]$ for differing central star masses M_{CS}, arbitrarily shifted with respect to $\log(T_B)$ (grey curves). It will be noted that the curves have closely similar profiles irrespective of M_{CS}. The dark solid curve corresponds to the mean trend employed in our present analysis.

3. THE EXPECTED VARIATION OF $N[\log(T_B)]$

Phillips (2003b) has recently investigated the variation to be expected in $N[\log(T_B), M_{CS}]$, the number of sources associated with a particular central star mass M_{CS}, and located within unit logarithmic interval of T_B. These functions are evaluated using the evolutionary tracks of Schönberner (1979;1981;1983) and Blocker & Schönberner (1990), and by making reasonable assumptions concerning shell expansion and optical depths.

Examples of these trends are illustrated in Figure 2, where we have overlaid the profiles expected for several central star masses (gray curves). There are small differences between the curves arising from evolutionary variations in $Q(\lambda < 912$ Å), the flux of H ionizing photons, and differences in numerical binning. Apart from this, however, it is apparent that all of the profiles are very closely similar. We find a sharp increase and peaking in $N[\log(T_B), M_{CS}]$ towards higher values of T_B, arising at the point at which H ionizing fluxes $Q(\lambda < 912$ Å) reach their maximum. This is followed by a decline over the range 0 $<\log(T_B) < 0.7$, corresponding to a decrease in H-burning within the central star, followed by a later increase resulting from optically thin expansion ($\log(T_B) < 0$). The shapes of the curves are therefore a consequence of both central star evolution and changes in shell opacity.

The positions of these profiles vary as a function of central star mass. Where $^{MAX}\ T_B$ is the temperature associated with the peak in $N[\log(T_B), M_{CS}]$,

for instance, then we find that

$$\log(^{MAX}T_B) = 27.65\ \log(M_{CS}) + 7.09\ , \quad (1)$$

for $-0.25 < \log(M_{CS}/M_\odot) < -0.15$. It follows that profiles $N[\log(T_B), M_{CS}]$ are shifted to high T_B where masses M_{CS} are large, and vice versa for lower values of mass.

Finally, it may be noted that the dark solid curve in Fig. 2 represents the mean trend in $N[\log(T_B)]$, evaluated on the basis of trends for 6 model central star profiles. This represents a reasonable approximation for most values of M_{CS}, and we shall employ it to fit observed trends in $N[\log(T_B)]$ (§ 4).

4. MODELLING THE VARIATIONS IN THE CENTRAL STAR MASS FUNCTION

We have modeled the trends in Fig. 1 using the mean synthetic function $N_{SYN}[\log(T_B), M_{CS}]$ illustrated in Fig. 2, and taking into account increasing opacities as T_B approaches 10^4 K. Specifically, the observed function $N_{OBS}[\log(T_B)]$ is related to the synthetic mass function $N(M_{CS})$ through

$$N_{OBS}[\log(T_B)]d\log T_B = \int_0^{M_{UP}} N(M_{CS})\times$$

$$\times N_{SYN}[\log(T_B), M_{CS}]\, dM_{CS}\, d\log T_b\ , \quad (2)$$

for any particular value of T_B, where M_{UP} is the upper limit central star mass, taken (in the present analysis) to equal the Chandrasekhar limit. Modelling of $N_{OBS}[\log(T_B)]$ then permits us to ascertain $N(M_{CS})$ to within fairly tight limits.

The fits between model and observed trends are illustrated for two cases in Fig. 2 ($|b_{LOW}| = 0°$ and $|b_{LOW}| = 5°$). We have also illustrated the fit between an $M_{CS} = 0.6\ M_\odot$ profile, and the observed trend for $|b_{LOW}| = 15°$ (see Figure 3). Two conclusions may be drawn from this latter comparison. The first is that the sharp peak in $N[\log(T_B)]$ is well represented in terms of a single mass function. This does not imply that all high latitude sources possess a single mass, but it does suggest that the range in masses is narrow, and that the absolute values of M_{CS} are low. The comparison between observed and theoretical trends appears tolerably good down to $\log(T_B) \sim 0$, below which there is an increasing disparity between the curves. It is likely that much of this latter difference arises from decreasing levels of source detection.

The theoretical mass functions required to achieve these fits are illustrated in Figures 4 and 5. They are estimated for sources within the range $1.0 < \log(TB) < 3.6$. It is clear, from these, that

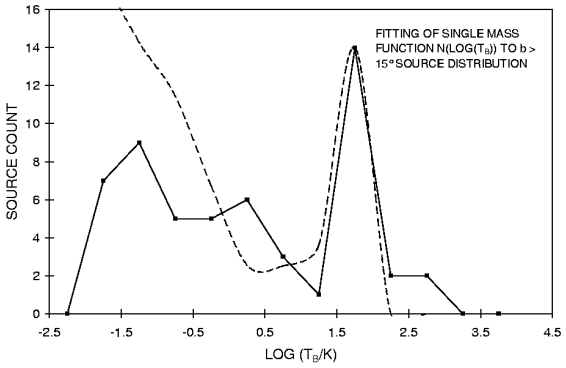

Fig. 3. The variation of $N[\log(T_B)]$ for sources having $b > 15°$ (solid lines). This has been fitted with the model trend for $M_{CS} = 0.6\ M_\odot$ (dashed lines). It will be seen that the fit is tolerably good down to $\log(T_B) \sim 0$, below which there is a growing disparity between the respective trends. It is likely that much (possibly all) of this disparity arises from the decreasing detectability of low T_B sources.

the mass function for all of the sources combined (i.e., $|b_{LOW}| = 0°$) appears to be relatively shallow (Fig. 4). The fall-off of $N(M_{CS})$ is much slower than either the Zhang & Kwok (1993) or Phillips (2001) mass functions, although it does appear to be comparable with that of Kaler & Jacoby (1991) for Magellanic Cloud planetaries. This difference between the functions is hardly surprising given the biases noted in § 2, and the fact that our function applies for higher brightness temperature sources alone. What is more critical, from the perspective of our present analysis, is the way in which $N(M_{CS})$ varies with latitude. This is illustrated in Fig. 5, whence it is clear that $N(M_{CS})$ steepens considerably as $|b_{LOW}|$ approaches 7.5°. It is apparent that by the time $|b_{LOW}| \sim 7.5°$, then most of the higher mass stars have "fallen out" of the functions, and that $N(M_{CS})$ peaks strongly about $M_{CS} \simeq 0.593\ M_\odot$. The typical error in the curves is probably of order $\Delta N(M_{CS})/N(M_{CS}) \sim 0.07$.

This trend may also be illustrated through the variation of mean central star masses $<M_{CS}>$ with $|b_{LOW}|$ (Figure 6). It is apparent, here again, that there is a marked decline in $<M_{CS}>$ as $|b_{LOW}|$ increases. Typical gradients appear to be of order $d<M_{CS}>/d|b_{LOW}| \simeq 2.0\times10^{-3}\ \ M_\odot\ \deg^{-1}$.

Finally, we note that mean distances of the sources are likely to be of order ~ 2.06 kpc where one adopts the statistical distances of Phillips (2002). This would imply an approximate gradient $dM_{CS}/d|z_{LOW}| \simeq 5.6\times10^{-2}\ \ M_\odot\ \mathrm{kpc}^{-1}$; where

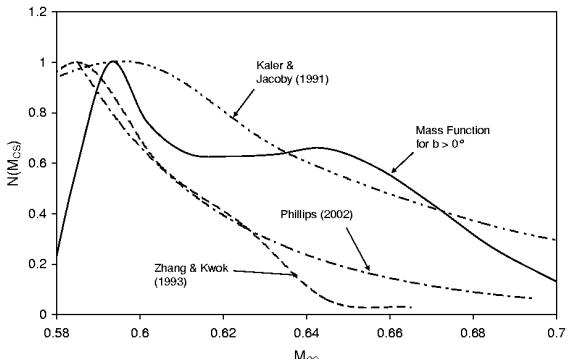

Fig. 4. A comparison between the central star mass function $N(M_{CS})$ for $|b_{LOW}| \geq 0°$, with various other functions taken from the published literature. It will be noted that although our present function is comparable to that of Kaler & Jacoby (1991), it falls-off much less steeply than those of Zhang & Kwok (1993) and Phillips (2001). All of these functions have been arbitrarily normalized.

$|z_{LOW}|$ is the counterpart of $|b_{LOW}|$, and corresponds to the lower limit height of nebulae above the Galactic plane. It should be emphasised that the distances to PNe are quite uncertain, however, and the latter values would be decreased by factors $\sim$ 2.7 where the distances of Zhang (1995) are employed.

Note, finally, that the accuracy of our conclusions depends upon the validity of our modeling. Variations in the commencement of shell optical

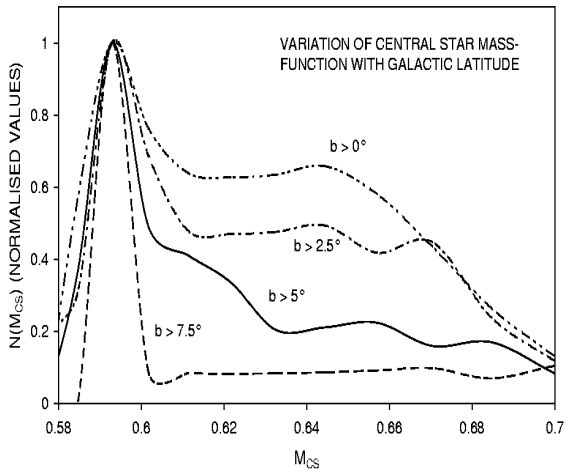

Fig. 5. Normalized mass functions for various lower limit latitudes. It will be seen that $N(M_{CS})$ varies appreciably as $|b_{LOW}|$ increases.

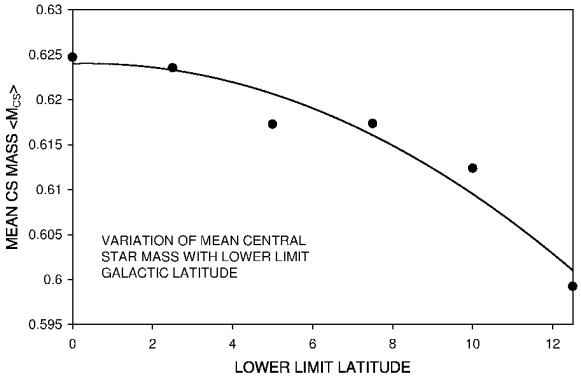

Fig. 6. The variation of mean central star mass $<M_{CS}>$ as a function of lower limit latitude $|b_{LOW}|$. The solid curve represents a second order polynomial least squares fit.

thinness, or the velocities of shell expansion may affect the shape and positioning of our profiles $N[\log(T_B), M_{CS}]$. To take just a few examples, acceleration or deceleration of the shells would lead to a broadening or narrowing of the profiles, as illustrated in Figure 7. This leads to a steepening or reduction of the gradients $dN(M_{CS})/dM_{CS}$. Similarly, a variation in ionization front velocities V_I from the value of 25 km s^{-1} adopted here would cause a bodily shift of the functions along the T_B axis. A velocity $V_I = 20$ km s^{-1}, for instance, would shift the functions $N[\log(T_B), M_{CS}]$ a distance $\Delta \log(T_B) \simeq -2 \log(V_I/25 \text{ km s}^{-1}) \simeq 0.2$ to larger values of T_B, and cause our functions $N(M_{CS})$ to shift $\Delta\ M_{CS} \simeq 0.01\ M_\odot$ to larger values of mass. Finally, we note that the so-called transition time, the period between when central stars leave the AGB and nebulae become appreciably ionized, is of uncertain duration. It may range from a few hundred to several thousands of years. Such a delay in the commencement of fully-fledged PNe evolution may have the effect of shifting mass functions $N(M_{CS})$ to lower values of M_{CS} (i.e., towards the left of the Figs. 5 and 6).

It is unlikely for the most part, however, that such changes will affect our conclusions. Thus we note that the comparison between our model and higher latitude results (Fig. 3) suggests that the synthetic functions are reasonably reliable —or at least, they appear to be so over the range for which observed trends can be trusted. Similarly, there is not the slightest doubt that actual profiles $N[\log(T_B), M_{CS}]$ shift in the way proposed here; that they move towards higher T_B where M_{CS} is large, and towards

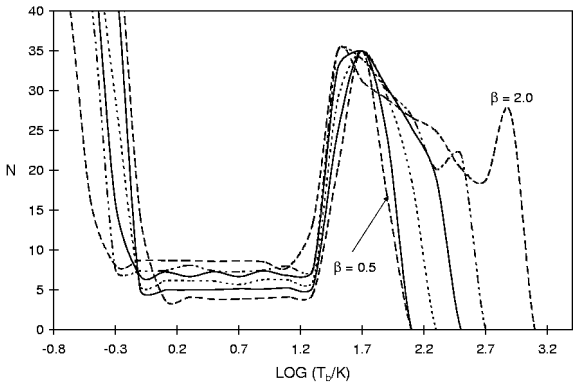

Fig. 7. The variation of $N[\log(T_B)]$ predicted for M_{CS} = 0.6 $M_\odot$. In this case, the ionization front velocities V_I are taken to vary with shell evolutionary time T_{EV} as $V_I \propto T_{EV}^{\beta-1}$. The various curves correspond (moving sequentially from the r.h.s. of the figure) to β = 2.0, 1.5, 1.25, 1.0, 0.75, and 0.5. It is apparent that I-front acceleration ($\beta > 1$) leads to broadening of the principal peak, whilst deceleration ($\beta < 1$) has the reverse effect.

lower T_B where the reverse is the case. The deduced variations in $N(M_{CS})$ are therefore likely to be qualitatively correct, even if the precise forms of these functions are open to revision.

It therefore seems that the observed variation of $N[\log(T_B)]$ with b is likely to reflect a variation of M_{CS} with z. A detailed analysis, of the kind assayed above, offers the prospect of placing stronger constraints on dM_{CS}/dz that has been possible heretofore. The conversion of M_{CS} to M_{PG}, using initial-final mass functions such as that of Weidemann (1987), may also permit us to evaluate Galactic gradients for nebular progenitor masses.

5. CONCLUSIONS

We have analyzed observed brightness temperatures for some 484 nebulae, and find that the distribution function $N[\log(T_B)]$ varies with Galactic latitude b. Whilst $N[\log(T_B)]$ appears to be broad where latitudes are small, it becomes very much more strongly peaked where values of b are large.

These various curves have been modeled using synthetic profiles $N[\log(T_B),\ M_{CS}]$, whence we are able to determine central star mass functions $N(M_{CS})$.

It seems likely that the proportion of high M_{CS} nebulae decreases as b increases, and that this causes corresponding changes in $<M_{CS}>$. We find that $d<M_{CS}>/d\,|b_{LOW}| \simeq 2.0\times10^{-3}$ $M_\odot$ deg^{-1}, implying that $d<M_{CS}>/d\,|z_{LOW}| \simeq 5.6\times10^{-2}$ $M_\odot$ kpc^{-1} (although this latter value depends upon which distance scale is employed, and may be up to three times smaller where the distances of Zhang (1995) are employed). Since M_{CS} is monotonically related to M_{PG}, the progenitor mass, then it follows that it should be possible to evaluate similar gradients for progenitor masses as well.

REFERENCES

Blocker, T., & Schönberner, D. 1990, A&A, 240, L11
Kaler, J. B., & Jacoby, G. H. 1991, ApJ, 382, 134
Koeppen, J., & Cuisinier, F. 1997, A&A, 319, 98
Marigo, P., Bressan, A., & Chiosi, C. 1998, A&A, 331, 564
Milne, D. K. 1979, A&AS, 36, 227
Milne, D. K., & Aller, L. H. 1975, A&A, 38, 183
_____. 1982, A&AS, 50, 209
Phillips, J. P. 2001, MNRAS, 326, 1041
_____. 2002, ApJS, 139, 199
_____. 2003a, MNRAS, 344, 501
_____. 2003b, A&A, in press
Renzini, A., & Voli, M. 1981, A&A, 94, 175
Schönberner, D. 1979, A&A, 79, 108
_____. 1981, A&A, 103, 119
_____. 1983, ApJ, 272, 708
van den Hoek, L. B., & Groenewegen, M. A. T. 1997, A&AS 123, 305
Weidemann, V. 1987, A&A, 188, 74
Zhang, C. Y. 1995, ApJS, 98, 659
Zhang, C. Y., & Kwok, S. 1993, ApJS, 88, 137
Zijlstra, A. A., Pottasch, S. R., & Bignell, C. 1989, A&AS, 79, 329

John Peter Phillips: Instituto de Astronomía y Meteorología, Av. Vallarta No. 2602, Col. Arcos Vallarta, 44130 Guadalajara, Jalisco, México. (jpp@cencar.udg.mx).